Facile approach to enhance the Pt utilization and CO-tolerance of Pt/C catalysts by physically mixing with transition-metal oxide nanoparticles†

Jingyu Xi,[ab] Jianshe Wang,[ab] Lihong Yu,[a] Xinping Qiu*[ab] and Liquan Chen[ab]

Received (in Cambridge, UK) 15th December 2006, Accepted 23rd January 2007
First published as an Advance Article on the web 8th February 2007
DOI: 10.1039/b618310g

A very simple and promising method to design the anode catalyst architecture for direct alcohol fuel cells by physically mixing Pt/C catalyst with transition-metal oxide nanoparticles is presented and electrochemical measurements confirm that this unique catalyst structure has excellent activity toward alcohol and CO electro-oxidation.

As is well known, direct alcohol fuel cells (DAFCs) have received increasing interest for their use as power sources for mobile applications.[1–3] However, two key problems still inhibit the commercialization of DAFCs. The first is the high cost of the precious metal Pt, and the second is the sluggish kinetics and catalyst poisoning caused by CO-like species. To solve the first problem, numerous researches have been focused on the reduction of Pt loading by increasing the catalyst specific active area and its accessibility.[4–9] For the second problem, advanced electro-catalyst design relies on the bifunctional mechanism, which means a second component, such as Ru, assists the oxidation of CO-like species by adsorption of oxygen-containing species nearby the poisoned Pt sites.[4,10] Also, several other Pt-based binary (PtRu, PtSn, *etc.*),[4,5,10] ternary (PtRuNi, PtRuIr, *etc.*),[11,12] and quaternary (PtRuOsIr, *etc.*)[13] catalysts have been reported to show good activity. Among all the reported catalysts, the PtRu-based system is recognized as the most promising candidate.[2–5] Recently, we reported a novel nanocomposite $Pt/RuO_2{\cdot}H_2O/CNT$ catalyst which showed excellent performance compared with the benchmark PtRu/C catalyst.[14] Unfortunately, the Ru element is also very expensive, which restricts the wide application of PtRu and/or $PtRuO_2{\cdot}H_2O$ based catalysts in DAFCs. Another strategy by using metal oxide (MO) modified (or coated) carbon black (CB) or carbon nanotube (CNT) as the support of Pt has also been developed, in which the MO can also enhance the CO tolerance of the catalysts, according to the bifunctional mechanism.[15,16] However, it is hard to control the size, shape, morphology, and thickness of the MO on the surface of CB. As a result, part of the Pt may be inactive due to poor contact with the CB support (Fig. S1, ESI†).

Herein, we present a novel concept to design the anode catalyst architecture for DAFCs by directly and physically mixing Pt/C catalyst with transition-metal oxide (TMO) nanoparticles. Although some researches have been done by mixing Pt/C with Ru/C,[17–19] our strategy is completely different. As shown in Scheme 1, TMOs are dispersed homogeneously in the interspaces of Pt/C nanoparticles, resulting in a high level of TMO-Pt–C interfaces, which greatly accelerates the electro-oxidation of CO_{ads} through a bifunctional approach. Electrochemical measurements confirm that this unique catalyst structure has excellent activity toward alcohol and CO electro-oxidation. In addition, the diluting effect of TMO nanoparticles in this catalyst structure permits ready access of reactant to the Pt/C catalyst and thereby enhances the utilization of Pt.

Several familiar TMO nanoparticles, which have been widely studied as catalysts or catalytic support for CO oxidation and the water–gas shift (WGS) reaction,[20–24] *i.e.* CeO_2, $ZrO_2$and TiO_2 (Fig. S2. ESI†), were tested in terms of their effect on the Pt/C catalyst. Commercial Pt/C (E-Tek, 20 wt% Pt) was used and is denoted as Pt/C. A catalyst ink was prepared by ultrasonic dispersion of Pt/C, as-prepared TMO nanoparticles, and Nafion ionomer in a mixed solution of ethylene glycol (EG) and ionized water. A gold patch (1 × 1 cm) coated with catalyst ink was used as the working electrode. A saturated calomel electrode (SCE) and a Pt gauze were used as reference and counter electrodes, respectively. All electrode potentials in this paper are referenced to the SCE.

Fig. S3(a) and (b), ESI,† show typical TEM images of Pt/C and as-prepared CeO_2 nanoparticles, respectively. The carbon support has an average particle size of about 30–40 nm while CeO_2 has an

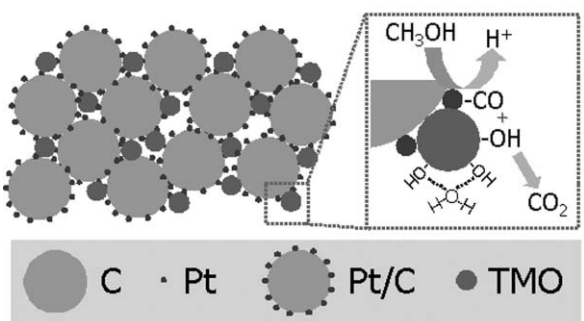

Scheme 1 Schematic representation of catalyst layer structure of Pt/C nanoparticles mixed with transition-metal oxide (TMO) nanoparticles. The right part shows the bifunctional mechanism of CO electro-oxidation. The adsorbed oxygen-containing species on the surface of TMO[20–24] can assist the oxidation of CO-like species which is adsorbed on the nearby Pt sites. (Nafion ionomer and electrons are not shown.)

[a]*Key Lab of Organic Optoelectronics and Molecular Engineering, Department of Chemistry, Tsinghua University, Beijing, 100084, China. E-mail: qiuxp@tsinghua.edu.cn; xijingyu@gmail.com; Fax: 86-10-62794234*
[b]*Lab of Advanced Power Sources, Graduate School at Shenzhen, Tsinghua University, Shenzhen, 518055, China*
† Electronic supplementary information (ESI) available: Experimental procedures and additional figures. See DOI: 10.1039/b618310g

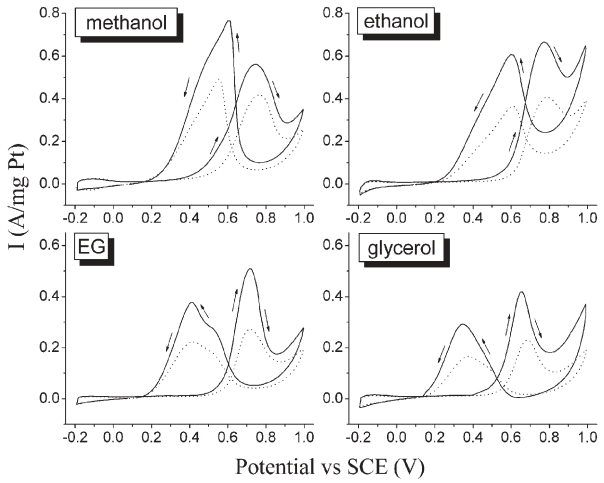

Fig. 1 Cyclic voltammetry curves of alcohol electro-oxidation at Pt/C (dotted line) and Pt/C + 20 wt% CeO_2 (solid line) at 25 °C in 1 mol L^{-1} alcohol–1 mol L^{-1} $HClO_4$ in the potential range −0.2 to 1.0 V *vs.* SCE with a scan rate of 50 mV s^{-1}. Only the 50th scan is shown and used for comparison of the catalytic activity of the specified catalysts.

average particle size of 9.5 nm. Fig. S3(c)–(g)† show SEM images and EDS analysis of the novel Pt/C + CeO_2 catalyst architecture. As can be seen from Fig. S3(d)–(g),† Pt/C particles, CeO_2 nanoparticles and Nafion ionomer can be dispersed homogeneously in the catalyst layer by the simple ultrasonic method.

Fig. 1 shows CV curves of alcohol electro-oxidation at Pt/C and Pt/C + 20 wt% CeO_2 catalysts. For all four alcohols, Pt/C + 20 wt% CeO_2 exhibits a much higher activity than pristine Pt/C. The peak current densities I_m (mA mg^{-1} Pt) at Pt/C + 20 wt% CeO_2 catalyst are about 1.35 (methanol), 1.64 (ethanol), 1.87 (EG), and 1.82 (glycerol) times that at Pt/C, respectively. Furthermore, the onset and peak potentials at Pt/C + 20 wt% CeO_2 are both lowered compared with those of Pt/C for all alcohols. In addition, almost no activity degradation was observed even after 500 cycles of uninterrupted scanning in 1 mol L^{-1} ethanol–1 mol L^{-1} $HClO_4$ solution (as shown in Fig. S4, ESI†), indicating the good stability of the Pt/C + CeO_2 catalyst nanoarchitecture in acid media.

Considering that the two catalysts have the same Pt loading (0.1 mg cm^{-2}), the significant enhancement on activity should be mainly due to the special catalyst structure resulting from the addition of CeO_2 nanoparticles. To clarify the role of CeO_2, the electrochemically active surface (EAS) and ethanol electro-oxidation activity of Pt/C catalyst with and without CeO_2 are compared in Table 1. The EAS of Pt/C increase from 58.1 m^2 g^{-1} Pt to 68.7 m^2 g^{-1} Pt by the addition of CeO_2 nanoparticles can be attributed to the dilution effect of CeO_2 nanoparticles in the novel catalyst structure (Scheme 1), which will permit ready access of alcohol reactant to the Pt/C catalyst and thereby enhance the utilization of Pt. More importantly, it can be seen from Table 1 that the specific peak current density I_s (mA cm^{-2} Pt) of ethanol electro-oxidation on Pt/C + 20 wt% CeO_2 is 0.98 mA cm^{-2} Pt, about 40% higher than that of pure Pt/C catalyst. We further believe that CeO_2 may promote the activity of Pt/C by accelerating the oxidation of CO_{ads} on the surface of Pt according to the bifunctional mechanism, as in the case of PtRu-based catalysts,[25–27] as shown in the right part of Scheme 1. Actually, this can be confirmed by the CO stripping voltammetry result.

As shown in Fig. 2, significant differences in the onset and peak potential for CO oxidation between the catalyst containing CeO_2 and that of pure Pt/C are observed, illustrating the beneficial role of CeO_2 for CO oxidation. Comparison of the CO oxidation curves for the CeO_2-containing catalyst reveals that the onset potential for Pt/C + 20 wt% CeO_2 is found at even lower potential (0.43 V) than that for Pt/C (0.51 V). The CO oxidation peak potential for Pt/C + 20 wt% CeO_2 (0.52 V) is also lower than that for Pt/C (0.59 V), due to CO oxidation on the interface of CeO_2–Pt/C.[16] According to the bifunctional mechanism, the OH_{ads} or oxygen-containing species on CeO_2[28,29] can transform CO-like poisoning species (CO_{ads}) on Pt to CO_2 (see Scheme 1), releasing the active sites on Pt for further electrochemical reaction, and hence, the activity of Pt/C catalyst toward alcohol electro-oxidation is greatly enhanced. In addition, we also find a very small CO oxidation peak at about 0.30 V for Pt/C + 20 wt% CeO_2, which can be attributed to the CO oxidation on the surface of CeO_2, in accord with the CO stripping voltammetry result on pure CeO_2 nanoparticles (see the inset of Fig. 2). The small CO oxidation current on pure CeO_2 can be explained by the poor electron conductivity of CeO_2 or weak CO adsorption ability on the surface of CeO_2.

Fig. 3 presents the chronoamperometric curves of CO_{ads} oxidation on Pt/C and Pt/C + 20 wt% CeO_2. For both potentials, the CO oxidation peak time for Pt/C + 20 wt% CeO_2 is obviously shorter than that for Pt/C, suggesting a faster CO oxidation kinetics[30] at Pt/C + 20 wt% CeO_2 catalyst, which is another evidence that CeO_2 plays an important role to enhance the performance of Pt/C catalyst.

We also studied the CO electro-oxidation ability of Pt/C catalyst mixed with ZrO_2 and TiO_2 nanoparticles, respectively (Fig. S5, ESI†). Both Pt/C + 20 wt%ZrO_2 and Pt/C + 20 wt%TiO_2 show lower onset and peak potential for CO oxidation compared to Pt/C, as in the case of Pt/C + 20 wt% CeO_2. This reveals that a series of TMO nanoparticles can be used to improve the activity of Pt/C catalyst.

In summary, our studies open a very simple and promising way to enhance the Pt utilization and the activity of traditional Pt/C

Table 1 Electrochemical active surface (EAS), ethanol electro-oxidation and CO-stripping data of Pt/C and Pt/C + 20 wt% CeO_2 catalysts

		Ethanol electro-oxidation[b]				CO-stripping[c]	
Catalyst	EAS[a] /m^2 g^{-1} Pt	E_{onset}/V	E_{peak}/V	I_s/mA cm^{-2} Pt	I_m/mA mg^{-1} Pt	E_{onset}/V	E_{peak}/V
Pt/C	58.1	0.46	0.79	0.71	412.3	0.51	0.59
Pt/C + 20 wt% CeO_2	68.7	0.29	0.77	0.98	676.2	0.43	0.52

[a] Calculated from the H_2 adsorption–desorption region in CV curves obtained at 1 M $HClO_4$ solution.[9] [b] Obtained from Fig. 1. [c] Obtained from Fig. 2.

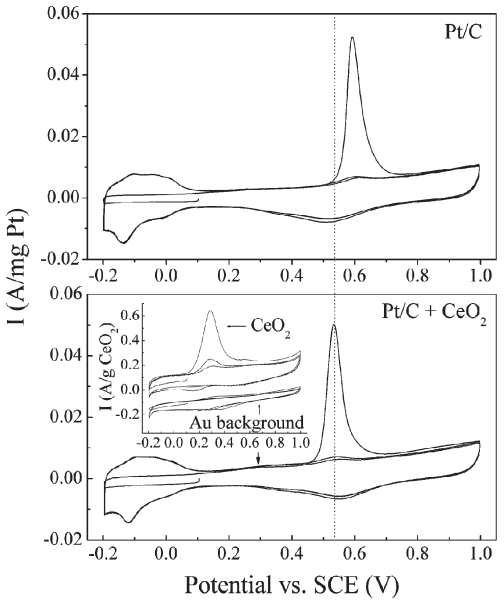

Fig. 2 CO stripping voltammetry curves recorded at 25 °C in 1 mol L^{-1} $HClO_4$ in the potential range −0.2 to 1.0 V *vs.* SCE with a scan rate of 10 mV s^{-1} for Pt/C and Pt/C + 20 wt% CeO_2. The CO was adsorbed at 0.1 V for 20 min; subsequently, the solution CO was removed by N_2 bubbling for 30 min maintaining at 0.1 V. The inset shows CO stripping voltammetry curve for pure CeO_2 nanoparticles and the background of a gold patch recorded at the same condition.

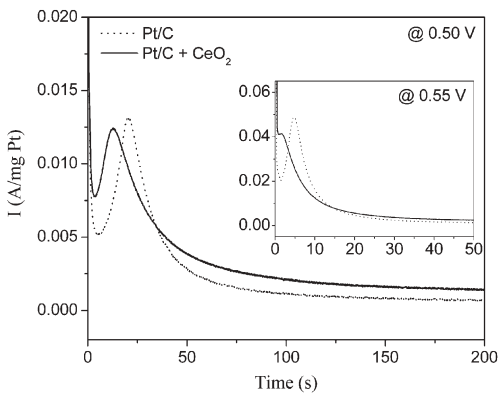

Fig. 3 Chronoamperometric curves of CO adlayer oxidation on Pt/C and Pt/C + 20 wt% CeO_2 recorded at 25 °C in 1 mol L^{-1} $HClO_4$ at different potentials. The CO was adsorbed at 0.1 V *vs.* SCE for 20 min; subsequently, the solution CO was removed by N_2 bubbling for 30 min maintaining at 0.1 V.

catalysts for alcohol and CO electro-oxidation by direct mixing of Pt/C catalyst with TMO nanoparticles. TMO nanoparticles can promote the oxidation of CO_{ads} on Pt according to the bifunctional mechanism as in the case of PtRu-based catalysts. Our preliminary results also show that this strategy can be successfully used to enhance the alcohol electro-oxidation activity of the state-of-the-art PtRu/C (E-TEK; 20 wt% on Vulcan, Pt : Ru = 1 : 1), Pt/CNT, and PtRu/CNT catalysts (Fig. S6, ESI†). These results will be reported in the near future. We believe that by optimizing the type, size, shape, crystal planes, and the ratio of the TMO nanoparticles, the performance of Pt/C catalyst for alcohol and CO electro-oxidation can be further improved and this work is now underway in our lab. In addition, this type of Pt/C + TMO catalyst nanoarchitecture may also find use as an anode catalyst for proton exchange membrane fuel cells (PEMFC) fed by reforming hydrogen which contains much more CO.

This work is supported by the National Natural Science Foundation of China (50606021, 90410002) and State Key Basic Research Program of China (2002CB211803).

Notes and references

1 B. C. H. Steele and A. Heinzel, *Nature*, 2001, **414**, 345.
2 R. Dillon, S. Srinivasan, A. S. Arico and V. Antonucci, *J. Power Sources*, 2004, **127**, 112.
3 S. Q. Song and P. Tsiakaras, *Appl. Catal., B*, 2006, **63**, 187.
4 K. Y. Chan, J. Ding, J. W. Ren, S. A. Cheng and K. Y. Tsang, *J. Mater. Chem.*, 2004, **14**, 505.
5 H. S. Liu, C. J. Song, L. Zhang, J. J. Zhang, H. J. Wang and D. P. Wilkinson, *J. Power Sources*, 2006, **155**, 95.
6 T. S. Ahmadi, Z. L. Wang, T. C. Green, A. Henglein and M. A. EI-Sayed, *Science*, 1996, **272**, 1924.
7 H. P. Liang, H. M. Zhang, J. S. Hu, Y. G. Guo, L. J. Wan and C. L. Bai, *Angew. Chem., Int. Ed.*, 2004, **43**, 1540.
8 W. Z. Li, C. H. Liang, W. J. Zhou, J. S. Qiu, Z. H. Zhou, G. Q. Sun and Q. Xin, *J. Phys. Chem. B*, 2003, **107**, 6292.
9 D. Zhao and B. Q. Xu, *Angew. Chem., Int. Ed.*, 2006, **45**, 4955.
10 A. Hamnett, *Catal. Today*, 1997, **38**, 445.
11 S. J. Liao, K. A. Holmes, H. Tsaprilis and V. I. Birss, *J. Am. Chem. Soc.*, 2006, **128**, 3504.
12 Y. M. Liang, H. M. Zhang, Z. Q. Tian, X. B. Zhu, X. L. Wang and B. L. Yi, *J. Phys. Chem. B*, 2006, **110**, 7828.
13 E. Reddington, A. Sapienza, B. Gurau, R. Viswanathan, S. Sarangapani, E. S. Smotkin and T. E. Mallouk, *Science*, 1998, **280**, 1735.
14 L. Cao, F. Scheiba, C. Roth, F. Schweiger, C. Cremers, U. Stimming, H. Fuess, L. Chen, W. Zhu and X. Qiu, *Angew. Chem., Int. Ed.*, 2006, **45**, 5315.
15 Y. X. Bai, J. J. Wu, J. Y. Xi, J. S. Wang, W. T. Zhu, L. Q. Chen and X. P. Qiu, *Electrochem. Commun.*, 2005, **7**, 1087.
16 J. Wang, J. Xi, Y. Bai, Y. Shen, J. Sun, L. Chen, W. Zhu and X. Qiu, *J. Power Sources*, 2007, **164**, 555.
17 M. Mazurek, N. Benker, C. Roth and H. Fuess, *Fuel Cells*, 2006, **6**, 208.
18 C. Roth, N. Martz, F. Hahn, J. M. Leger, C. Lamy and H. Fuess, *J. Electrochem. Soc.*, 2002, **149**, E433.
19 J. Kaiser, L. Colmenares, Z. Jusys, R. Mortel, H. Bonnemann, G. Kohl, H. Modrow, J. Hormes and R. J. Behm, *Fuel Cells*, 2006, **6**, 190.
20 K. Zhou, X. Wang, X. Sun, Q. Peng and Y. Li, *J. Catal.*, 2005, **229**, 206.
21 E. Aneggi, J. Llorca, M. Boaro and A. Trovarelli, *J. Catal.*, 2005, **234**, 88.
22 T. X. T. Sayle, S. C. Parker and D. C. Sayle, *Phys. Chem. Chem. Phys.*, 2005, **7**, 2936.
23 M. Comotti, W. Li, B. Spliethoff and F. Schuth, *J. Am. Chem. Soc.*, 2006, **128**, 917.
24 C. M. Y. Yeung, K. M. K. Yu, Q. J. Fu, D. Thompsett, M. I. Petch and S. C. Tsang, *J. Am. Chem. Soc.*, 2005, **127**, 18010.
25 M. Watanabe and S. Motoo, *J. Electroanal. Chem.*, 1975, **60**, 267.
26 F. Maillard, G. Q. Lu, A. Wieckowski and U. Stimming, *J. Phys. Chem. B*, 2005, **109**, 16230.
27 C. Roth, N. Benker, Th. Buhrmester, M. Mazurek, M. Loster, H. Fuess, D. C. Koningsberger and D. E. Ramaker, *J. Am. Chem. Soc.*, 2005, **127**, 14607.
28 O. Pozdnyakova, D. Teschner, A. Wootsch, J. Krohnert, B. Steinhauer, H. Sauer, L. Toch, F. C. Jentoft, A. Knop-Gericke, Z. Paal and R. Schlogl, *J. Catal.*, 2006, **237**, 1.
29 O. Pozdnyakova, D. Teschner, A. Wootsch, J. Krohnert, B. Steinhauer, H. Sauer, L. Toch, F. C. Jentoft, A. Knop-Gericke, Z. Paal and R. Schlogl, *J. Catal.*, 2006, **237**, 17.
30 M. Arenz, K. J. J. Mayrhofer, V. Stamenkovic, B. B. Blizanac, T. Tomoyuki, P. N. Ross and N. M. Markovic, *J. Am. Chem. Soc.*, 2005, **127**, 6819.

Electronic Supplementary Information

Facile approach to enhance the Pt utilization and CO-tolerance of Pt/C catalyst by physically mixing with transition metal oxides nanoparticles

Jingyu Xi,[a,b] Jianshe Wang,[a,b] Lihong Yu,[a] Xinping Qiu*[a,b] and Liquan Chen[a,b]

[a] Key Lab of Organic Optoelectronics and Molecular Engineering, Department of Chemistry, Tsinghua University, Beijing 100084, China. E-mail: qiuxp@tsinghua.edu.cn (X. Qiu), xijingyu@gmail.com (J. Xi); Fax: 86-10-62794234

[b] Lab of Advanced Power Sources, Graduate School at Shenzhen, Tsinghua University, Shenzhen 518055, China.

Experimental Section

Preparation of transition metal oxides (TMO) nanoparticles

All transition metal oxides (TMO) nanoparticles used in this work were prepared by molten salt method as described in Ref. (1) and (2). Cerium nitrate, zirconium nitrate, and tetrabutyl titanate were used as precursors for preparation of CeO_2, ZrO_2, and TiO_2, respectively. For a typical synthesis process, $K_2C_2O_4$ solution was added drop-wise into the cerium nitrate solution with constant stirring to attain a pH value of 10. The resultant precipitation was filtrated and washed with deionized water and ethanol repeatedly, and then dried at 80 ^oC for 12 h. This precipitation and KNO_3 were mixed with a mortar and pestle at molar ratio of 1:3. The mixtures were calcined at 500 ^oC for 3 h, and then cooled to ambient temperature. The products were immersed in deionized water, washed and filtered repeatedly to remove the residual fluxes. Finally, the products were dried at 120 ^oC to obtain the CeO_2 nanoparticles. The morphologies of the TMO nanoparticles were examined by TEM (JEOL model JEM-1200EX). As shown in Figure S2, the average particle size is 9.5 nm, 4.6 nm, and 10.1 nm for CeO_2, ZrO_2, and TiO_2, respectively.

Working electrode preparation

The catalyst ink was prepared by mixing the Pt/C catalyst (E-Tek, 20 wt.% Pt) with perfluorsulfonic acid solution (5 wt.%, Nafion®, DuPont), ethylene glycol (EG) and deionized water ultrasonically. For the case of Pt/C+TMO, TMO nanoparticles were first dispersed in deionized water ultrasonically, and then mixed with Pt/C, Nafion®, and

EG ultrasonically. The resulting slurry was spreaded onto a gold patch of ca. 1.0 cm^2 (1×1 cm). Then the electrode was dried at 80 ^oC in air with the total catalyst loadings of about 0.1 mg Pt/cm^2.

Characterization

The morphologies of the Pt/C catalyst and TMO nanoparticles were examined by TEM (JEOL model JEM-1200EX). The catalyst structure of Pt/C+TMO was observed using a scanning electron microscope (SEM, LEO1530), and EDS analysis was used to analyze the element distribution in the catalyst architecture.

Electrochemical measurements

Electrochemical measurements were carried out in a three electrode cell using a Solartron SI1287 workstation at 25 ºC. A saturated calomel electrode (SCE) and Pt gauze were used as reference and counter electrodes, respectively. All electrode potentials in this paper are referred to the SCE. A solution of in 1 M alcohol + 1 M $HClO_4$ was used as electrolyte. All the reagents used were of analytical grade. Several activation scans were performed until reproducible voltammograms were obtained. Cyclic voltammograms were recorded in the potential range -0.2 to 1.0 V vs. SCE at a scan rate of 50 mV s^{-1}. The oxidation of preadsorbed CO was measured by CO stripping voltammetry in 1M $HClO_4$ solution at a scan rate of 10 mV s^{-1}. All the recorded currents are corrected for the weight percentage of the platinum in catalysts. The experimental error during CV test in this work is within 5 mV.

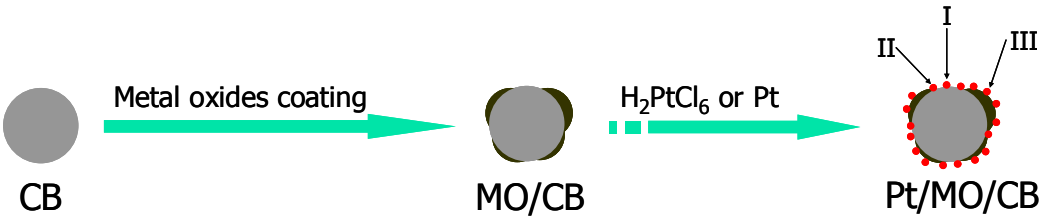

Figure S1 Schematic representation of the preparation process of Pt/MO/C catalyst. First, metal oxide (MO) was coated on the surface of carbon black (CB) by microwave irradiation method[3] or co-precipitation method[4] to obtain the MO/CB support. It is hard to control the size, shape, morphology, and thickness of the MO on the surface of CB in this step. Secondly, Pt nanoparticles were deposited on MO/CB to obtain the Pt/MO/CB catalyst. Three types of Pt species exit in the Pt/MO/CB catalyst, as shown in the figure.

(I) Pt deposits on the surface of CB, which is the same as pristine Pt/C catalyst.

(II) Pt deposits on the interface of CB and MO, which causes the most active site of the catalyst, when Pt contact well with CB and MO. According to the bifunctional mechanism, the OH_{ads} species on MO can transform CO-like poisoning species (CO_{ads}) on Pt to CO_2, releasing the active sites on Pt for further electrochemical reaction.

(III) Pt deposits on the surface of MO, which may be useless due to the bad electron conductivity of MO.

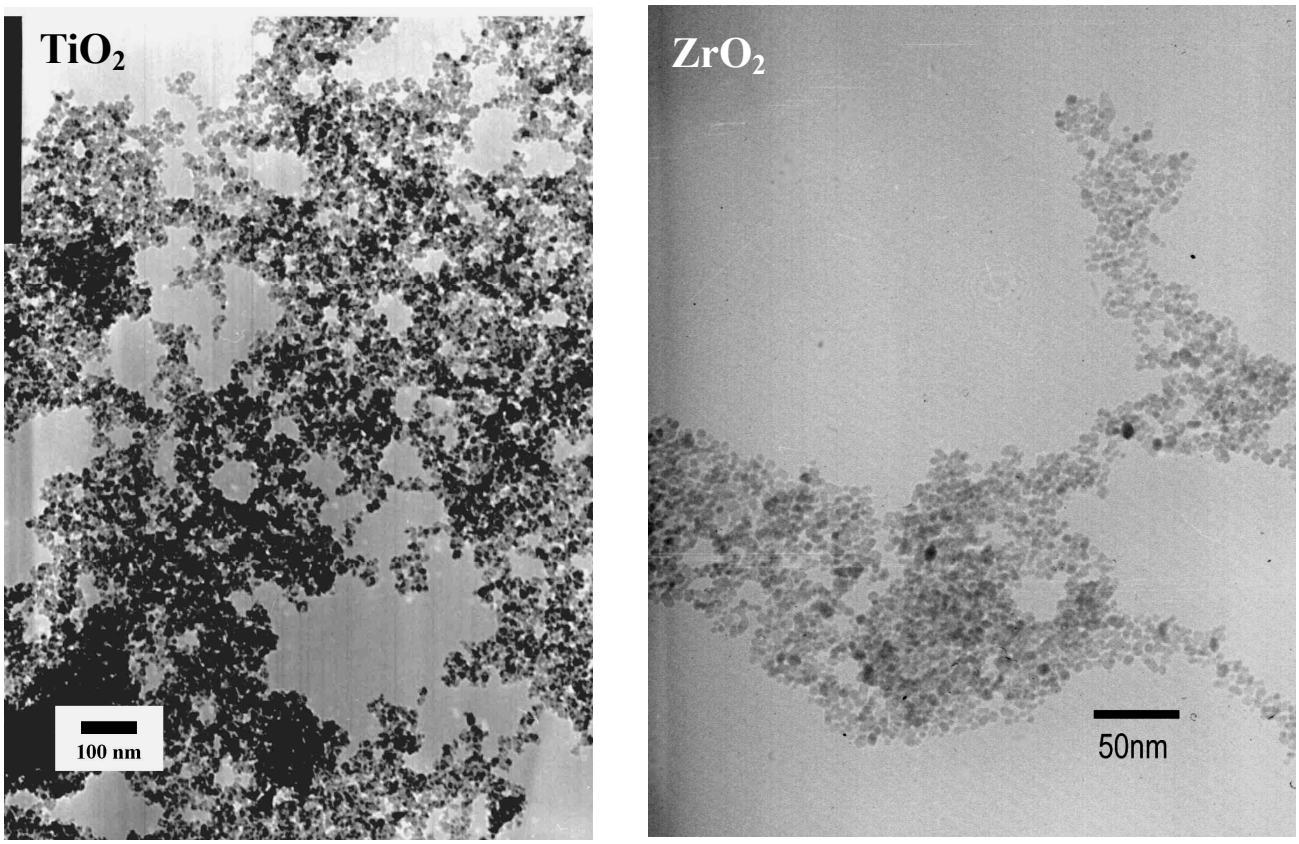

Figure S2 TEM images of TiO_2 (left) and ZrO_2 (right) nanoparticles prepared from molten salt method. The average particle size is 10.1 nm and 4.6 nm for TiO_2 and ZrO_2, respectively.

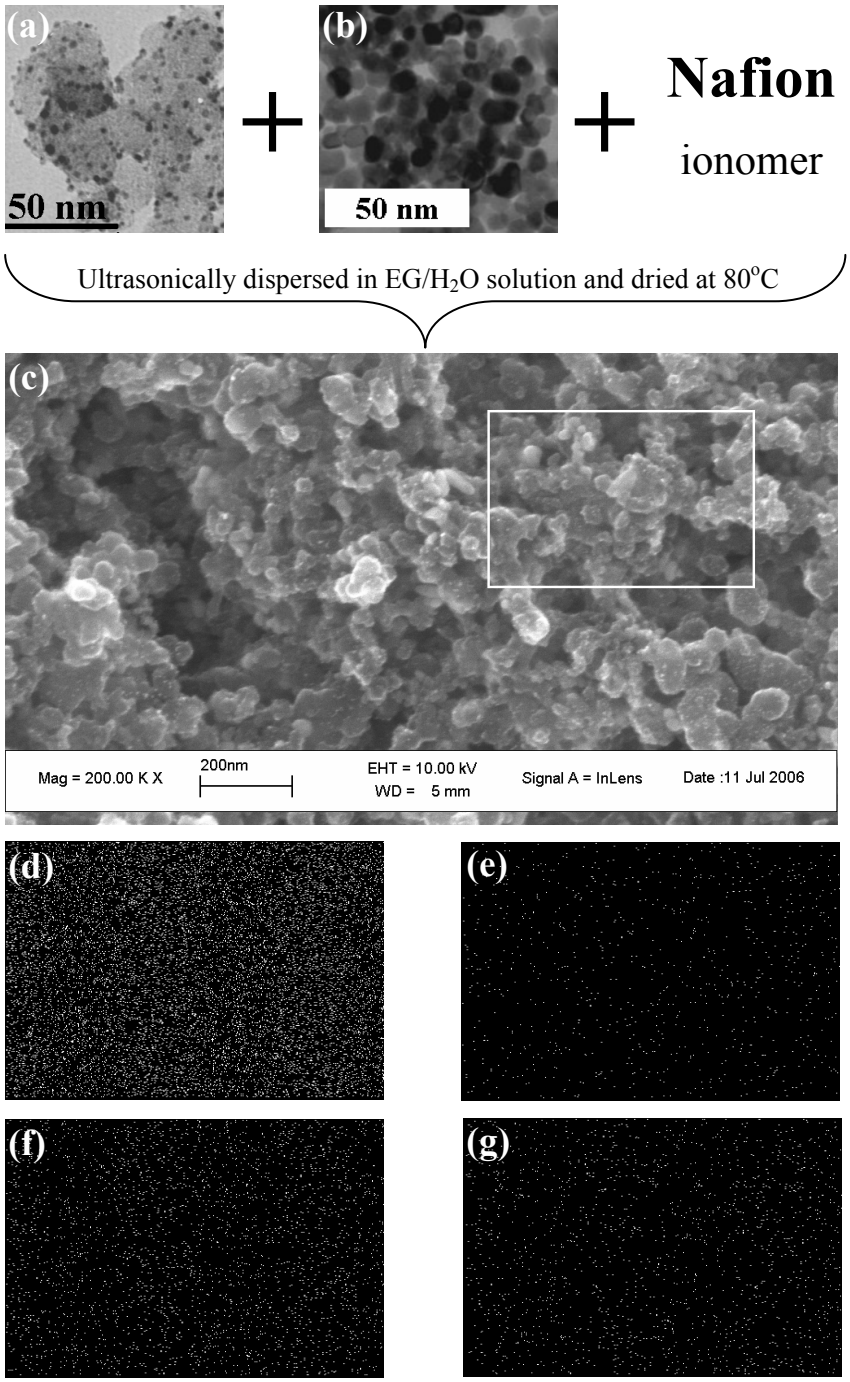

Figure S3. (a) TEM image of Pt/C (E-Tek, 20 wt.% Pt) catalyst; (b) TEM image of as prepared CeO_2 nanoparticles; (c) SEM image of the catalyst architecture of Pt/C+20wt.%CeO_2; (d)-(g) show the distribution of C, Pt, Ce, S element of the selective position in (c), which was measured by EDS, respectively.

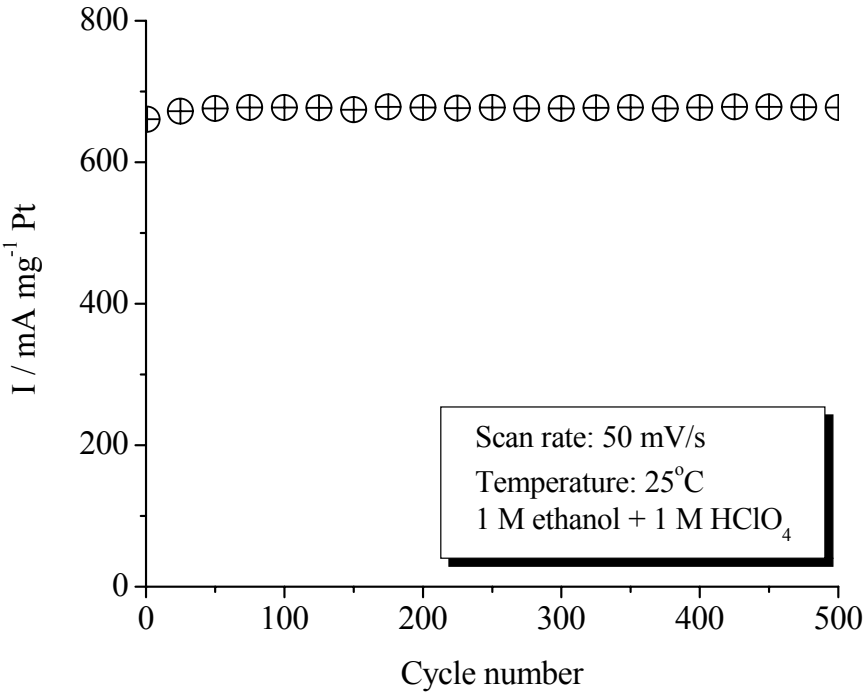

Figure S4. Stability of the Pt/C+20wt.%CeO_2 catalyst over 500 cycles of ethanol electrooxidation.

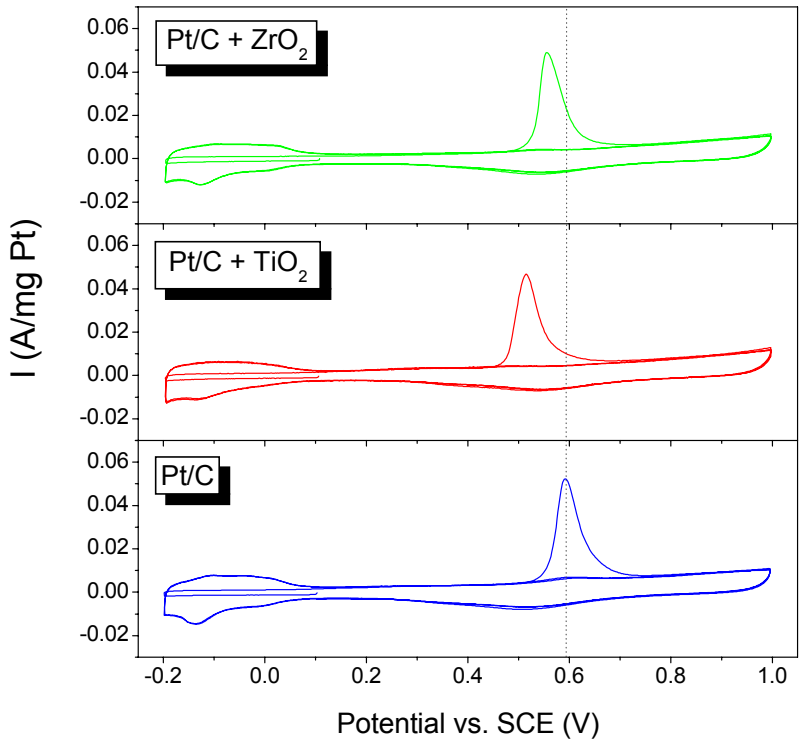

Figure S5. CO stripping voltammetry curves recorded at 25 ^{o}C in 1 mol/L $HClO_4$ in the potential range of -0.2 V to 1.0 V vs. SCE with a scan rate of 10 mV/s for Pt/C, Pt/C+20wt.%ZrO_2, and Pt/C+20wt.%TiO_2 catalysts. The CO was adsorbed at 0.1 V for 20 min, subsequently, the solution CO was removed by N_2 bubbling for 30 min maintaining at 0.1 V. Both Pt/C+20wt.%ZrO_2 and Pt/C+20wt.%TiO_2 show lower onset and peak potentials for CO oxidation compared with pristine Pt/C catalyst.

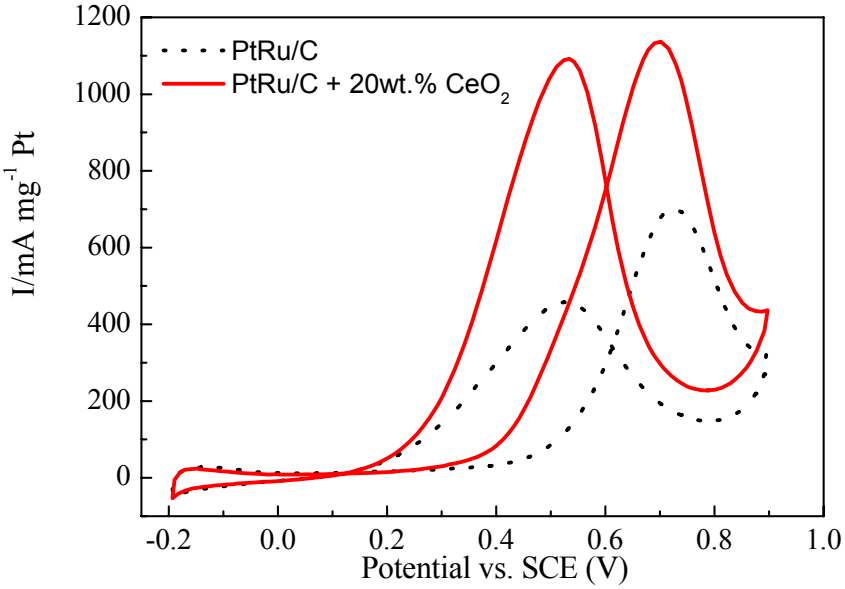

Figure S6. Cyclic voltammetry curves of methanol electro-oxidation at PtRu/C (E-TEK; 20 wt% on Vulcan, Pt:Ru=1:1) with and without CeO_2 nanoparticles recorded at 25 ^oC in 1 M methanol + 1 M $HClO_4$ in the potential range of -0.2 V to 0.9 V vs. SCE with a scan rate of 50 mV/s. Only the last voltammograms (the 50th scan) were used for comparison the catalytic activity of the specified catalysts.

References

(1) Liang H. Y.; Qiu X. P.; Zhang S. C.; He Z. Q.; Zhu W. T.; Chen L. Q. *Electrochem. Commun.* **2004**, *6*, 505-509.

(2) Liang H. Y.; Qiu X. P.; Chen H.L.; He Z. Q.; Zhu W. T.; Chen L. Q. *Electrochem. Commun.* **2004**, *6*, 789-794.

(3) Xu C. W.; Shen P. K. *J. Power Sources* **2005**, *142*, 27-29.

(4) Bai Y. X.; Wu J. J.; Xi J. Y.; Wang J. S.; Zhu W. T. Chen L. Q.; Qiu X. P. *Electrochem. Commun.* **2005**, *7*, 1087-1090.